Published in final edited form as:
*Cancer Res*. 2010 December 1; 70(23): 9693–9702. doi:10.1158/0008-5472.CAN-10-2286.

# Combining ATR suppression with oncogenic Ras synergistically increases genomic instability, causing synthetic lethality or tumorigenesis in a dosage-dependent manner

**Oren Gilad**[1], **Barzin Y. Nabet**[1], **Ryan L. Ragland**[1], **David W. Schoppy**[1], **Kevin D. Smith**[1], **Amy C. Durham**[2], and **Eric J. Brown**[1,*]

[1] Abramson Family Cancer Research Institute and the Department of Cancer Biology, University of Pennsylvania School of Medicine, Philadelphia, PA 19104

[2] School of Veterinary Medicine, Philadelphia, PA 19104

## Abstract

Previous studies indicate that oncogenic stress activates the ATR-Chk1 pathway. Here, we demonstrate that ATR-Chk1 pathway engagement is essential for limiting genomic instability following oncogenic Ras transformation. ATR pathway inhibition in combination with oncogenic Ras expression synergistically increased genomic instability, as quantified by chromatid breaks, sister chromatid exchanges and H2AX phosphorylation. This level of instability was significantly greater than that observed following ATR suppression in untransformed control cells. In addition, consistent with a deficiency in long-term genome maintenance, hypomorphic ATR pathway reduction to 16% of normal levels was synthetic lethal with oncogenic Ras expression in cultured cells. Notably, elevated genomic instability and synthetic lethality following suppression of ATR were not due to accelerated cycling rates in Ras-transformed cells, indicating that these synergistic effects were generated on a per-cell-cycle basis. In contrast to the synthetic lethal effects of hypomorphic ATR suppression, subtle reduction of ATR expression (haploinsufficiency) in combination with endogenous levels of K-ras$^{G12D}$ expression elevated the incidence of lung adenocarcinoma, spindle cell sarcoma and thymic lymphoma in p53 heterozygous mice. K-ras$^{G12D}$-induced tumorigenesis in ATR$^{+/-}$p53$^{+/-}$ mice was associated with intrachromosomal deletions and loss of wild-type p53. These findings indicate that synergistic increases in genomic instability following ATR reduction in oncogenic Ras-transformed cells can produce two distinct biological outcomes: synthetic lethality upon significant suppression of ATR expression and tumor promotion in the context of ATR haploinsufficiency. These results highlight the importance of the ATR pathway both as a barrier to malignant progression and as a potential target for cancer treatment.

### Keywords

Ras; ATR; Chk1; p53; oncogenic stress; therapy

[*]To whom correspondence should be addressed: Eric J. Brown, Abramson Family Cancer Research Institute and the Department of Cancer Biology, University of Pennsylvania School of Medicine, 421 Curie Boulevard, Philadelphia, PA 19104, Phone: 215-746-2805, Fax: 215-573-2486, brownej@mail.med.upenn.edu.

Disclosure of Potential Conflicts of Interest
None

## Introduction

Hyperproliferative stimuli, oncogenic stress and tumor progression are associated with elevated genomic instability and DNA damage checkpoint signaling (1–8). Checkpoint signaling is regulated in large part by the ATR and ATM protein kinases, which serve as initial responders to aberrant replication fork progression and DNA double strand breaks, respectively (9–10). Checkpoint activation in these contexts has been proposed to function as a barrier to malignant progression by both preventing proliferation and countering the untoward effects of oncogenic stress on DNA metabolism and integrity (2–3,8).

Activation of the ATR pathway by oncogenic stress has been attributed to a variety of cellular changes, including premature or redundant origin firing, changes in inter-origin distance, and increased oxidative DNA damage (4–12). In both yeast and vertebrates, ATR signaling plays a critical role in maintaining genome stability following irregularities in DNA replication fork progression. Inhibition of polymerase processivity (e.g. reduced catalysis or encounters with damaged bases) and other disruptions that uncouple DNA unwinding from nucleotide incorporation activate ATR, which prevents replication fork collapse into DNA double strand breaks (9–10,13–22). In accord with this function, chromatid breaks at common fragile sites and other difficult-to-replicate regions of the genome are particularly increased when partial polymerase inhibition is combined with suppression of the ATR-Chk1 pathway (9,17–19,23). Notably, oncogenic stress alone has also been shown to increase breakage at common fragile sites (2–3,8), implying that suppression of the ATR-Chk1 pathway in this context may further elevate genomic instability in a synergistic fashion.

Herein, we investigate the hypothesis that oncogenic transformation produces an increased reliance on the ATR-Chk1 pathway to maintain genome stability. We demonstrate that ATR-Chk1 pathway inhibition in combination with expression of oncogenic forms of Ras elevates double strand break formation and mitotic recombination on a per-cell-cycle basis. Importantly, oncogene-induced dependence on the ATR pathway to maintain genome stability leads to distinct effects following ATR suppression: either promoting oncogenic Ras-induced tumorigenesis when ATR is haploinsufficient, or causing synthetic lethality when the ATR-Chk1 pathway is inhibited more substantially. These results demonstrate the importance of the ATR-Chk1 pathway in maintaining genomic stability under oncogenic stress and imply a key role for ATR suppression in both cancer etiology and treatment.

## Materials and Methods

### Oncogenic Ras-transformed cell line generation

Murine embryonic fibroblasts (MEFs) were immortalized via lentiviral introduction of shRNAs targeting $p16^{INK4A}$ and $p19^{ARF}$ (TRCN77813). Oncogenic Ras was expressed 1) by treatment of K-$ras^{G12D/+}$Cre-$ERT2^{+}$ MEFs with 0.2 μmol/L 4-hydroxytamoxifen (4-OHT, Calbiochem) for 48 hours (K-$ras^{G12D}$ endogenous levels), or 2) by infection of NIH3T3 cells (clone 7) or immortalized MEFs with recombinant retrovirus expressing K-$ras^{G12D}$ or H-$ras^{G12V}$. Control cell lines were produced in parallel using retrovirus derived from the corresponding empty vectors (pWZL-hygro or pBabe-puro). Infected cells were selected in 2 μg/mL puromycin (pBABE-puro vectors) or 200 μg/mL hygromycin (pWZL-hygo vectors) for 4–7 days to enrich for transduced cells.

### Cell culture and lentiviral infections

For all experiments, cells were cultured in defined growth media [DMEM supplemented with bovine pancreatic insulin (10 μg/mL, Sigma), transferrin (10 μg/mL, Calbiochem), HDL (10 μg/mL, Lee Biosolutions), recombinant murine EGF (50 ng/mL, Millipore),

glutamine (2 mmol/L, Gibco), HEPES pH 7.4 (10 mmol/L, Gibco), and 0.5% fetal bovine serum (FBS, Hyclone)], similar to previously described conditions (24–25). ShATR (H1UG1 vector) and other shRNA-expressing lentiviruses were produced and titered as described (21). For shRNA lentivirus infections, $2.5\times10^5$ cells were plated on 10 cm plates and infected with concentrated virus at an MOI of 10–20, typically yielding 95–98% transduction. BrdU labeling (45 min) was used to quantify of S phase representation as described (21).

### Immunoblotting

Whole cell lysates in 1X SDS lysis buffer (10% glycerol, 79 mmol/L SDS, 62.5 mmol/L Tris pH 6.8) were separated by SDS-PAGE (15% for H2AX; 10% for Chk1 and GAPDH) and blotted onto 0.45 μm PVDF membranes. Blots were detected for phospho-S239 H2AX (Upstate, JBW301 clone), GAPDH (US Biological), ATR (Santa Cruz), phospho-S345 Chk1 (Cell Signaling) and total Chk1 (Santa Cruz) according to manufacturer instructions.

### Mitotic spreads and detection of chromatid breaks and sister chromatid exchange

Mitotic spreads were prepared as previously described following a 3–4 hour treatment with 0.5 μmol/L nocodazole (19,21). To detect and quantify sister chromatid exchanges, cells were incubated with 10 μmol/L BrdU (Sigma) for two cell doublings and subsequently arrested in mitosis via nocodazole treatment. Mitotic spreads were prepared, processed and stained with Giemsa, and photographed using a 100X objective lens. Quantification of chromatid breaks and SCEs were performed using double blind methods.

### Tumorigenesis in LSL-K-ras$^{G12D}$ mice and histological analysis

LSL-K-ras$^{G12D}$ (26–27), Cre-ERT2$^{+}$ (28), p53$^{+/-}$ (*tm1Tyj*) and ATR$^{+/-}$ (13) mice were intercrossed to produce the indicated genotypes (background: 129SvEv/C57BL/6 mixed). Tamoxifen (20 mg/ml in 98% corn oil:2% ethanol) was administered via a single intraperitoneal injection at a dose of 0.3 mg (15 μl). Mice were monitored until death or when euthanized in accord with IACUC endpoint criteria. Following necropsy, tissues were fixed in 4% paraformaldehyde (PFA) in phosphate buffered saline at 4°C overnight, dehydrated, and embedded in paraffin. For gross histological examination of lung tissue, 5 micron serial sections were generated and the tenth section of each series was mounted and stained with hematoxylin and eosin (H&E) for histopathological evaluation. Classification of pulmonary lesions was performed as described (29). Noted pathologies were tracked across nearby stained sections (50 microns apart) and quantified per lung by double-blind methods. Immunohistochemical detection of p53 was performed on fixed tumor samples following antigen unmasking in 10.9 mmol/L citric acid and inactivation of endogenous peroxidases with hydrogen peroxide. Incubation with anti-p53 antibodies (Novocastra; NCL-p53-CM5p, 1:100, 4°C overnight) was followed by detection with goat anti-rabbit (1:100) HRP-conjugated secondary antibodies (1hr at RT) and DAB staining. Slides were washed and stained for two minutes with hematoxylin prior to mounting and visualization.

### Quantitative PCR

Applied Biosystems' Primer Express Software 3.0 was utilized for design of quantitative PCR primer and MGB probe sets to detect the wild-type p53 and unrecombined LSL-K-ras$^{G12D}$ alleles (Supplemental Table 1). For p53 allele quantification, primer and probe sets detected intronic sequences between exons 6 and 7 of wild-type p53, a region deleted within the p53-null allele. For detection of mosaic lox recombination of the LSL-K-ras$^{G12D}$ allele, primer and probe sets (26) were used to amplify and detect sequences in the transcriptional stop element and flanking a single loxP site. Quantitative PCR was performed with genomic DNA as a template; amplification and detection were performed using TaqMan Universal

PCR Master Mix (Applied Biosystems) on an Applied Biosystems 7900HT Sequence Detection System. Primer sets for regional quantification of chromosome 11 (Supplemental Table 1) were designed using the Primer3Plus program (UCSC), and quantitative PCR of tumor and tail genomic DNA was performed using SYBR Green PCR Master Mix (Applied Biosystems). Amplification of GAPDH was used as an endogenous control for all ΔΔ CT analyses.

### Array-based Comparative Genomic Hybridization (CGH)

Mouse genome CGH microarrays (180,000 oligos per array, 4 arrays per chip, Agilent Technologies) were custom designed using eArray software (Agilent Technologies) with genomic regions represented at 500 bp intervals within the p53 locus, and at 50 kb intervals throughout the remainder of the mouse genome. Genomic DNA from tumor and tamoxifen-untreated tail tissue was utilized for fluorescent probe generation (500 ng DNA per probe). Reciprocal labeling and hybridization of tumor and normal DNA on two independent arrays per tumor sample were performed (dye-swap) using Cy3 and Cy5 fluorophors. Arrays were scanned with Agilent Scanner Control software following manufacture instructions (Agilent Technologies). Analysis of scanned images from CGH two-color oligonucleotide arrays were performed using Partek Genomics Suite version 6.5 (Partek Inc.).

## Results

### Oncogenic Ras transformation creates an increased reliance on the ATR-Chk1 pathway to maintain genome integrity

Engagement of the ATR-Chk1 pathway maintains genome stability in response to irregularities in the progression of DNA replication (9,15–22). Because hyperactive growth factor signaling and oncogenic stress have each been shown to activate the ATR-Chk1 pathway in human cells (2–7), we hypothesized that ATR-Chk1 activation under these conditions may provide an important genome stabilizing function. To examine the effect of ATR-Chk1 pathway inhibition in combination with oncogene-transformation, mouse embryonic fibroblast cell lines were generated that expressed K-ras$^{G12D}$ or H-ras$^{G12V}$. Ras-expression led to phenotypes characteristic of transformation, including increased ERK phosphorylation, morphological changes, loss of contact inhibition at confluence, and the ability to produce tumors following transplantation into immunocompromised mice (data not shown).

The ability of oncogenic Ras expression to activate the ATR-Chk1 pathway in murine cells was confirmed by quantification of Chk1 phosphorylation on S345, an ATR kinase substrate. These studies were performed under defined growth-factor conditions that have been previously shown to ameliorate the genome destabilizing effects of cell culture and, in subconfluent cultures, cause cell cycling rates to be similar between untransformed and oncogene-expressing cells (24–25). In agreement with previous reports (2–7), a significant increase in Chk1 phosphorylation was observed in all oncogenic Ras-expressing cell lines in comparison to untransformed controls (Fig. 1A). Activation of Chk1 by Ras transformation ranged from 150% of control levels under endogenous expression of K-ras$^{G12D}$ to a three- to ten-fold increase following overexpression of K-ras$^{G12D}$ or H-ras$^{G12V}$.

Because Chk1 phosphorylation by ATR is stimulated to low levels during normal S phase progression (ref. 9–10 and data not shown), it was conceivable that increased Chk1 phosphorylation in H-ras$^{G12V}$-transformed cells was the product of a proportionate increase of cells in S phase. However, arguing against this possibility, the percentage of H-ras$^{G12V}$-transformed cells in S phase was either similar to untransformed controls or elevated insufficiently to account for the fold increase in Chk1 phosphorylation (Fig. 1A). Notably,

the level of Chk1 phosphorylation observed in H-ras$^{G12V}$-transformed cells was similar to that stimulated by treatment of control cells with 0.23 μmol/L aphidicolin (Fig. 1B and C), a concentration of DNA polymerase inhibitor that only partially impedes nucleotide incorporation (18). In aggregate, these studies demonstrate that oncogenic Ras activates the ATR pathway in a manner that is compatible with continued DNA synthesis and is not the product of increased S phase representation or accelerated proliferation rates (Figs. 1 and 3A).

Irregularities in DNA synthesis have been previously shown to cause an increased reliance on the ATR pathway to suppress double strand break generation (9,18–19,21–22). We reasoned that H-ras$^{G12V}$-transformation might similarly create a dependence on ATR-Chk1 pathway activation to maintain genome integrity. To test this hypothesis, the effect of inhibiting the ATR-Chk1 pathway on genome integrity in H-ras$^{G12V}$-transformed cells and untransformed controls was quantified using three hallmarks of genomic instability: H2AX phosphorylation, sister chromatid exchange (SCE), and chromatid breaks.

ATR deficiency in combination with exogenous DNA polymerase inhibition (e.g. aphidicolin treatment) has previously been shown to stimulate ATM/DNA-PK-dependent phosphorylation of H2AX in response to increased double strand break formation (19,21). Similarly, ATR/Chk1 pathway inhibition in combination with H-ras$^{G12V}$ expression cells elevated H2AX phosphorylation to significantly higher levels than produced in control cells (Fig. 2A). Such synergistic increases were observed using hypomorphic suppression of ATR expression to 15.7% of normal levels (± 3.8% standard error, S.E.) and following short-term inhibition of Chk1 kinase activity (3-hour Gö6976 treatment, Fig. 2A). These greater-than-additive increases in H2AX phosphorylation was observed in multiple independent Ras-transformed cell lines following ATR suppression (data not shown). Therefore, H-ras$^{G12V}$ expression increases reliance on the ATR-Chk1 pathway to prevent H2AX phosphorylation during otherwise unperturbed cell cycle progression.

Consistent with an increase in double strand breaks and subsequent recombinatorial repair, sister chromatid exchange (SCE) rates in ATR-suppressed H-ras$^{G12V}$-transformed cells were significantly elevated over those observed in control cells (Fig. 2B and D). Importantly, because the SCE staining procedure measures recombination frequencies precisely within two consecutive rounds of replication, increased SCE rates in oncogenic Ras-transformed cells cannot be due to elevated representation of S phase or increased cell cycling rates. The ability of short-term Chk1 inhibition to induce H2AX phosphorylation in Ras-transformed cells (Fig. 2A) is consistent with this interpretation. These findings indicate that ATR-Chk1 pathway inhibition in combination with oncogenic stress leads to an increased utilization of DNA repair responses, and that such elevated rates of recombination are manifested within the context of individual cell cycles.

We next examined whether the combination of ATR suppression with oncogenic stress was sufficient to overwhelm compensatory DNA repair responses (Fig. 2A and B) and lead to increased chromatid breaks in M phase. Chromosome spreads were collected from H-ras$^{G12V}$-transformed and control cells after shRNA-mediated ATR suppression. Remarkably, suppressed expression of ATR in oncogenic Ras-transformed cells led to a highly synergistic increase in chromatid breaks over that observed in control cells (Fig. 2C and D). This synergistic effect may be produced both by elevated double strand break formation (Fig. 2A) and by cell cycle checkpoint deficiency, which allows increased transmission of breaks into M phase (19). Similar increases in chromosome breaks were observed using a distinct shRNA that targets ATR (Supplemental Fig. 2A and B). Notably, a portion of these breaks were observed at the Fra14A2 and Fra8E1 common fragile sites (FHIT and WWOX, respectively, data not shown), consistent with activation of the ATR

pathway serving an important role in suppressing common fragile site breakage under oncogenic stress. In aggregate, these data demonstrate that ATR pathway activation is relied upon to maintain genome stability under conditions of oncogenic stress.

Increased chromatid breaks in M phase predict several potential biological outcomes, depending on the level of ATR reduction. Because genomic instability was synergistically elevated when ATR suppression was combined with oncogenic stress (Fig. 2), significant suppression of ATR to hypomorphic levels might drive genomic instability to intolerable levels in Ras-transformed cells, while leaving untransformed counterparts relatively intact. Alternatively, ATR deficiency might sufficiently compromise cell cycle control to permit continued proliferation of Ras-transformed cells, despite increased genomic instability. Similarly, subtle reduction of ATR expression, such as haploinsufficiency, might either be sufficient to suppress tumorigenesis initiated by K-ras or accelerate malignant progression through a variety of mechanisms, including increased genomic instability and tumor suppressor gene loss. These possibilities were tested, as described below.

## Hypomorphic ATR pathway suppression is synthetic lethal with oncogenic Ras expression

As described above, significant reduction of ATR expression might 1) synergize with Ras-driven oncogenic stress to generate a level of genomic instability that is incompatible with continued cell proliferation (synthetic lethality), or 2) suppress cell cycle checkpoint control and permit the continued proliferation of genetically unstable cells. To test these hypotheses, shRNA-mediated targeting was used to reduce ATR expression to 16% of normal levels in H-ras$^{G12V}$-transformed cells and untransformed controls (Figs. 2 and 3) and cell proliferation was measured. Within the first four days of culture, hypomorphic ATR suppression did not significantly affect the proliferation of Ras-transformed or control lines (Fig. 3A and B), consistent with ineffectual cell cycle checkpoint responses to the instability observed at day 2 (Fig. 2).

However, by six to eight days, the proliferation of H-ras$^{G12V}$-transformed cells was potently suppressed by reduced ATR expression, ultimately leading to diminished cell numbers (Fig. 3A). The suppressed proliferation of H-ras$^{G12V}$-transformed cells was at least partly due to an increased rate of cell death, based on the elevated frequency of cells with sub-G1 DNA content (Fig. 3C and D). Importantly, although hypomorphic ATR suppression ultimately limited the proliferation of both cell types (Fig. 3A, C and D), the anti-proliferative effect of ATR reduction on H-ras$^{G12V}$-transformed cells was significantly greater than that observed on similarly-treated untransformed controls (Fig. 3A, $P = 0.03$; Fig. 3D, $P = 0.01$). This selective effect was also observed using a distinct shRNA that targets ATR expression (Supplemental Fig. 2C). Notably, under these sub-confluent conditions, Ras-transformed and untransformed controls proliferated similarly when wild-type levels of ATR were expressed (shCTRL-expressing cells, Fig. 3A). These data indicate that the effect of ATR suppression on proliferation of Ras-transformed cells is not simply the product of an increased number of cell cycles in the absence of full ATR expression but, rather, reflects increased instability on a per-cell-cycle basis.

## ATR haploinsufficiency promotes K-ras$^{G12D}$-induced tumorigenesis and p53 loss of heterozygosity (LOH)

Because ATR-Chk1 activation is increased in the presence of oncogenic stress and during neoplastic transformation, it has been proposed that ATR and other DNA damage response genes may serve as barriers to oncogene-driven tumorigenesis (2–8). Indeed, somatic mutations in ATR-Chk1 pathway components have been observed in human cancers and have been proposed to act as driver mutations in lung adenocarcinoma, endometrial carcinoma, and other cancers (30–37). Many of the mutations thus far characterized are

predicted to result in only partial ATR-Chk1 pathway reduction (28,30–32,35,37). However, according to our findings (Figs. 2 and 3), ATR haploinsufficiency in combination with oncogenic stress might either limit tumorigenesis via synthetic lethality, or promote it through a variety of mechanisms, including increased genomic instability and accelerated tumor suppressor gene loss.

To test the effect of haploinsufficient ATR expression (13) on oncogene-induced tumorigenesis, K-ras$^{G12D}$ expression was induced to endogenous levels in wild-type, ATR$^{+/-}$, p53$^{+/-}$ and ATR$^{+/-}$p53$^{+/-}$mice (Fig. 4A). Induction of K-ras$^{G12D}$ was accomplished by mosaic lox recombination of LSL-K-ras$^{G12D}$ knock-in allele (27) in a broad range of tissues through tamoxifen-mediated activation of a ubiquitously-expressed Cre-ERT2 fusion protein (28). Using this method, recombination of the lox-stop-lox element of K-ras$^{G12D}$ knock-in allele ranged from 10–23% in analyzed tissues, as determined by quantitative PCR (qPCR) on genomic DNA, and was not significantly affected by ATR haploinsufficiency (Fig. 4B).

Mouse survival following K-ras$^{G12D}$ expression was predominantly limited by oral papillomas, which forced euthanasia due to decreased food intake, and by myeloproliferation (Fig. 4C and Supplemental Fig. 3). These previously noted phenotypes (38-40) were not affected either by ATR or p53 haploinsufficiency, leading to similar median survival times for the genotypes analyzed, ranging from 54–81 days. However, upon necropsy, additional tumor types were revealed and found to occur at an increased frequency in ATR$^{+/-}$p53$^{+/-}$ mice compared to p53$^{+/-}$ mice (Fig. 4C and D). These tumors included thymic lymphomas (CD4$^{+}$, CD8$^{+}$) and subcutaneous spindle cell sarcomas (Fig. 4C), each of which were greater than 0.8 cm in diameter at the time of necropsy. Moreover, a significant increase in the appearance of lung nodules was observed in ATR$^{+/-}$p53$^{+/-}$ (Fig. 4C and D).

K-ras$^{G12D}$ expression has been shown to be sufficient to stimulate the generation of lung hyperplasias and several distinct varieties of lung adenoma; however, adenocarcinomas are most strongly induced in the absence of p53 (26,38,41–42). To examine the effect of ATR haploinsufficiency on incidence of these pathologies, lungs from ATR$^{+/-}$p53$^{+/-}$ and p53$^{+/-}$ animals were serial sectioned and quantified for lung adenomas and adenocarcinomas. Although the incidence of several common adenoma subtypes were unchanged by ATR heterozygosity, adenocarcinomas were observed exclusively in ATR$^{+/-}$p53$^{+/-}$ animals, indicating that ATR haploinsufficiency promotes the generation of this malignant form of lung cancer (Fig. 4E,Supplemental Fig. 4 and data not shown). Solid and mixed adenomas with atypia, which may represent preneoplasia (29), were also observed in ATR$^{+/-}$p53$^{+/-}$ and not detected in p53$^{+/-}$ controls (Fig. 4E). Together, these results demonstrate that ATR haploinsufficiency can act as a modifier of K-ras$^{G12D}$-induced tumorigenesis in mice.

The increased tumorigenesis in ATR$^{+/-}$p53$^{+/-}$ mice in comparison to p53$^{+/-}$ controls suggested that ATR haploinsufficiency might drive tumorigenesis through p53 LOH. To examine this possibility, two procedures were performed: immunocytochemical detection of p53 protein (Fig. 5A), and real-time qPCR quantification of the wild-type p53 allele in isolated genomic DNA from tumors (Fig. 5B). As expected based on tumor incidence, oral papillomas and myelocyte hyperproliferation were not associated with p53 LOH. However, the tumor types observed at increased incidence in ATR heterozygous animals had a relatively high frequency of p53 loss (Fig. 5B). This loss was generally characterized by intrachromosomal deletions in mouse chromosome 11 that encompassed the wild-type *Trp53* locus at 69.4 Mb, as determined by array CGH and qPCR analysis (Fig. 5C and D). In aggregate, these data indicate that ATR haploinsufficiency promotes K-ras$^{G12D}$-induced

tumorigenesis in a manner that correlates with increased intrachromosomal deletion of the p53 tumor suppressor gene.

## Discussion

Herein, we demonstrate that expression of oncogenic Ras in combination with ATR suppression leads to synergistic increases in genomic instability. Increased instability was not simply the consequence of increased S phase representation or elevated cycling rates following Ras transformation but, rather, was reflective of a greater dependence on the ATR pathway on a per-cell-cycle basis (Figs. 1–3). Synergistic increases in genomic instability produced two distinct biological outcomes in the context of oncogenic Ras expression: synthetic lethality upon substantial reduction of ATR expression (>80%) and tumor promotion in the context of ATR haploinsufficiency. These findings indicate that, while haploinsufficient loss of ATR may subtly elevate genomic instability and, thus, accelerate oncogene-driven carcinogenesis, further inhibition of the ATR-Chk1 pathway can drive genomic instability to intolerable levels and suppress proliferation.

The effect of ATR haploinsufficiency in promoting K-ras$^{G12D}$-induced tumorigenesis supports a growing body of evidence indicating a functional role for mutations in ATR pathway components in human carcinogenesis. Somatic mutations in ATR have been identified in colon, stomach and endometrial cancers (30–32,35), and may influence lung adenocarcinoma progression (33–34). In addition, a variant of Rad9, a component of the ATR-Chk1 pathway (9), has been shown to be strongly associated with increased risk of non-small cell lung cancer in humans (37). Mutations within a similar region in an *S. cerevisae* ortholog of human Rad9 (*S. cerevisase* Ddc1) disrupts checkpoint signaling in response to DNA damage, suggesting that the human Rad9 variant may be functionally compromised (43). Indeed, mutation or suppression of Chk1 has been noted in colon, stomach and endometrial cancers, and select B-cell lymphomas (30–31,35). These genetic association studies in humans are consistent with findings indicating that suppression of ATR-Chk1 pathway components promotes tumorigenesis in select tumor models (13,44–46).

According to our studies, the stimulatory effect of ATR-Chk1 pathway haploinsufficiency on tumorigenesis may be potently influenced by the increased reliance on ATR-Chk1 function produced by oncogenic stress (Figs. 1 and 2). Along these lines, ATR-Chk1 pathway haploinsufficiency may drive tumorigenesis either through subtle alleviation of cell cycle control or increased genome destabilization (Fig. 2). Notably, the expected low levels of genomic instability caused by ATR haploinsufficiency appear to promote the complete loss of non-essential tumor suppressor genes, such as p53 (Fig. 5), which may ultimately suppress checkpoint function more effectively than ATR haploinsufficiency alone. These findings may be useful in correlating tumor suppressor gene loss with candidate genetic modifiers in genome-wide association studies of human cancers. Moreover, detection of ATR-Chk1 pathway mutations may provide relevant prognostic indicators (47) and assist in choosing effective cancer treatment strategies, which could include inhibition of the ATR-Chk1 pathway, as discussed below.

Chk1 has previously been proposed to be a potential target for cancer treatment, most notably in combination with p53 deficiency (48). Indeed, Chk1 inhibitors are currently in Phase I and II clinical trials for the treatment of a variety of solid and hematologic malignancies (36,48–49). The studies described herein support the use of ATR-Chk1 pathway inhibition in cancer therapy. Because ATR phosphorylates a variety of DNA damage response intermediates in addition to Chk1 and selective Chk1 inhibition ultimately causes ATR activation (9–10,50), it is not known whether ATR inhibition will be identical

in efficacy to Chk1 suppression in cancer treatment. Nevertheless, each kinase plays an important role in replication fork stabilization (9–10), which is potentially the key function required for genome maintenance in the context of oncogenic stress and other conditions. Given the deleterious effect of complete ATR-Chk1 pathway ablation on normal tissue homeostasis (28), a critical determinant of the utility of this treatment will be identifying the genetic characteristics of cancers that cause selective sensitization to partial ATR-Chk1 inhibition.

Oncogenic Ras mutations are observed frequently in human cancers and are associated with some of the currently least treatable malignancies, including pancreatic, lung, ovarian, and colon cancer. Thus, ATR-Chk1 pathway inhibition may provide therapeutic opportunities where few alternatives are available. Many of the cancers associated with expression of oncogenic Ras also harbor mutations in p53, which as mentioned above is reported to produce an increased sensitivity ATR-Chk1 pathway inhibition (36,48–49). Along these lines, the greatest effect of ATR-Chk1 inhibition in cancer treatment may be achieved through the combined effects of these genetic interactions (e.g. p53 loss and oncogenic stress) and others, including somatic mutations within the ATR-Chk1 pathway (30–37) or other DNA damage response genes, e.g. ATM and H2AX (21,34,42). Thus, it is conceivable that malignancies harboring such combined genetic characteristics may be prime candidates for treatments utilizing ATR-Chk1 pathway inhibition.

## Supplementary Material

Refer to Web version on PubMed Central for supplementary material.

## Acknowledgments

We are indebted to Amma Asare, Yaroslava Ruzankina, Sara Small, Kathleen Haines, Richard Carroll, Douglas Lin, Alan Diehl, and the AFCRI Histology Core for methodological expertise and technical assistance. We are also grateful to the following for providing essential reagents: Tyler Jacks and David Tuveson (LSL-K-ras$^{G12D}$ mice) and J. Alan Diehl and Martine Roussel (pBabe-H-ras$^{G12V}$) and the Amy Golden Uleis memorial fund (purchase of pWZL-K-ras$^{G12D}$, Addgene, Inc.)

Grant Support

These studies were supported by the National Institute on Aging (R01AG027376), the Abramson Family Cancer Research Institute, and the V Foundation. O.G. was supported by an NIH training grant (R25CA101871).

## References

1. Denko NC, Giaccia AJ, Stringer JR, Stambrook PJ. The human Ha-ras oncogene induces genomic instability in murine fibroblasts within one cell cycle. Proc Natl Acad Sci U S A 1994;91:5124–5128. [PubMed: 8197195]
2. Gorgoulis VG, Vassiliou LV, Karakaidos P, et al. Activation of the DNA damage checkpoint and genomic instability in human precancerous lesions. Nature 2005;434:907–913. [PubMed: 15829965]
3. Bartkova J, Horejsi Z, Koed K, et al. DNA damage response as a candidate anti-cancer barrier in early human tumorigenesis. Nature 2005;434:864–870. [PubMed: 15829956]
4. Di Micco R, Fumagalli M, Cicalese A, et al. Oncogene-induced senescence is a DNA damage response triggered by DNA hyper-replication. Nature 2006;444:638–642. [PubMed: 17136094]
5. Bartkova J, Rezaei N, Liontos M, et al. Oncogene-induced senescence is part of the tumorigenesis barrier imposed by DNA damage checkpoints. Nature 2006;444:633–637. [PubMed: 17136093]
6. Fikaris AJ, Lewis AE, Abulaiti A, Tsygankova OM, Meinkoth JL. Ras triggers ataxia-telangiectasia-mutated and Rad-3-related activation and apoptosis through sustained mitogenic signaling. J Biol Chem 2006;281:34759–34767. [PubMed: 16968694]

7. Dominguez-Sola D, Ying CY, Grandori C, et al. Non-transcriptional control of DNA replication by c-Myc. Nature 2007;448:445–451. [PubMed: 17597761]
8. Halazonetis TD, Gorgoulis VG, Bartek J. An oncogene-induced DNA damage model for cancer development. Science 2008;319:1352–1355. [PubMed: 18323444]
9. Paulsen RD, Cimprich KA. The ATR pathway: fine-tuning the fork. DNA Repair (Amst) 2007;6:953–966. [PubMed: 17531546]
10. Cimprich KA, Cortez D. ATR: an essential regulator of genome integrity. Nat Rev Mol Cell Biol 2008;9:616–627. [PubMed: 18594563]
11. Davidson IF, Li A, Blow JJ. Deregulated replication licensing causes DNA fragmentation consistent with head-to-tail fork collision. Mol Cell 2006;24:433–443. [PubMed: 17081992]
12. Moiseeva O, Bourdeau V, Roux A, Deschenes-Simard X, Ferbeyre G. Mitochondrial dysfunction contributes to oncogene-induced senescence. Mol Cell Biol 2009;29:4495–4507. [PubMed: 19528227]
13. Brown EJ, Baltimore D. ATR disruption leads to chromosomal fragmentation and early embryonic lethality. Genes Dev 2000;14:397–402. [PubMed: 10691732]
14. Myung K, Datta A, Kolodner RD. Suppression of spontaneous chromosomal rearrangements by S phase checkpoint functions in Saccharomyces cerevisiae. Cell 2001;104:397–408. [PubMed: 11239397]
15. Tercero JA, Diffley JF. Regulation of DNA replication fork progression through damaged DNA by the Mec1/Rad53 checkpoint. Nature 2001;412:553–557. [PubMed: 11484057]
16. Lopes M, Cotta-Ramusino C, Pellicioli A, et al. The DNA replication checkpoint response stabilizes stalled replication forks. Nature 2001;412:557–561. [PubMed: 11484058]
17. Cha RS, Kleckner N. ATR homolog Mec1 promotes fork progression, thus averting breaks in replication slow zones. Science 2002;297:602–606. [PubMed: 12142538]
18. Casper AM, Nghiem P, Arlt MF, Glover TW. ATR regulates fragile site stability. Cell 2002;111:779–789. [PubMed: 12526805]
19. Brown EJ, Baltimore D. Essential and dispensable roles of ATR in cell cycle arrest and genome maintenance. Genes Dev 2003;17:615–628. [PubMed: 12629044]
20. Byun TS, Pacek M, Yee MC, Walter JC, Cimprich KA. Functional uncoupling of MCM helicase and DNA polymerase activities activates the ATR-dependent checkpoint. Genes Dev 2005;19:1040–1052. [PubMed: 15833913]
21. Chanoux RA, Yin B, Urtishak KA, et al. ATR and H2AX cooperate in maintaining genome stability under replication stress. J Biol Chem 2009;284:5994–6003. [PubMed: 19049966]
22. Smith KD, Fu MA, Brown EJ. Tim-Tipin dysfunction creates an indispensible reliance on the ATR-Chk1 pathway for continued DNA synthesis. J Cell Biol 2009;187:15–23. [PubMed: 19805627]
23. Durkin SG, Arlt MF, Howlett NG, Glover TW. Depletion of CHK1, but not CHK2, induces chromosomal instability and breaks at common fragile sites. Oncogene 2006;25:4381–4388. [PubMed: 16732333]
24. Loo DT, Fuquay JI, Rawson CL, Barnes DW. Extended culture of mouse embryo cells without senescence: inhibition by serum. Science 1987;236:200–202. [PubMed: 3494308]
25. Woo RA, Poon RY. Activated oncogenes promote and cooperate with chromosomal instability for neoplastic transformation. Genes Dev 2004;18:1317–1330. [PubMed: 15175263]
26. Jackson EL, Willis N, Mercer K, et al. Analysis of lung tumor initiation and progression using conditional expression of oncogenic K-ras. Genes Dev 2001;15:3243–3248. [PubMed: 11751630]
27. Tuveson DA, Shaw AT, Willis NA, et al. Endogenous oncogenic K-ras(G12D) stimulates proliferation and widespread neoplastic and developmental defects. Cancer Cell 2004;5:375–387. [PubMed: 15093544]
28. Ruzankina Y, Pinzon-Guzman C, Asare A, et al. Deletion of the developmentally essential gene ATR in adult mice leads to age-related phenotypes and stem cell loss. Cell Stem Cell 2007;1:113–126. [PubMed: 18371340]

29. Nikitin AY, Alcaraz A, Anver MR, et al. Classification of proliferative pulmonary lesions of the mouse: recommendations of the mouse models of human cancers consortium. Cancer Res 2004;64:2307–2316. [PubMed: 15059877]
30. Menoyo A, Alazzouzi H, Espin E, et al. Somatic mutations in the DNA damage-response genes ATR and CHK1 in sporadic stomach tumors with microsatellite instability. Cancer Res 2001;61:7727–7730. [PubMed: 11691784]
31. Vassileva V, Millar A, Briollais L, Chapman W, Bapat B. Genes involved in DNA repair are mutational targets in endometrial cancers with microsatellite instability. Cancer Res 2002;62:4095–4099. [PubMed: 12124347]
32. Lewis KA, Mullany S, Thomas B, et al. Heterozygous ATR mutations in mismatch repair-deficient cancer cells have functional significance. Cancer Res 2005;65:7091–7095. [PubMed: 16103057]
33. Davies H, Hunter C, Smith R, et al. Somatic mutations of the protein kinase gene family in human lung cancer. Cancer Res 2005;65:7591–7595. [PubMed: 16140923]
34. Greenman C, Stephens P, Smith R, et al. Patterns of somatic mutation in human cancer genomes. Nature 2007;446:153–158. [PubMed: 17344846]
35. Lewis KA, Bakkum-Gamez J, Loewen R, et al. Mutations in the ataxia telangiectasia and rad3-related-checkpoint kinase 1 DNA damage response axis in colon cancers. Genes Chromosomes Cancer 2007;46:1061–1068. [PubMed: 17879369]
36. Lapenna S, Giordano A. Cell cycle kinases as therapeutic targets for cancer. Nat Rev Drug Discov 2009;8:547–566. [PubMed: 19568282]
37. Tanaka Y, Maniwa Y, Bermudez VP, et al. Nonsynonymous single nucleotide polymorphisms in DNA damage repair pathways and lung cancer risk. Cancer 2010;116:896–902. [PubMed: 20052722]
38. Johnson L, Mercer K, Greenbaum D, et al. Somatic activation of the K-ras oncogene causes early onset lung cancer in mice. Nature 2001;410:1111–1116. [PubMed: 11323676]
39. Braun BS, Tuveson DA, Kong N, et al. Somatic activation of oncogenic Kras in hematopoietic cells initiates a rapidly fatal myeloproliferative disorder. Proc Natl Acad Sci U S A 2004;101:597–602. [PubMed: 14699048]
40. Chan IT, Kutok JL, Williams IR, et al. Conditional expression of oncogenic K-ras from its endogenous promoter induces a myeloproliferative disease. J Clin Invest 2004;113:528–538. [PubMed: 14966562]
41. Fisher GH, Wellen SL, Klimstra D, et al. Induction and apoptotic regression of lung adenocarcinomas by regulation of a K-Ras transgene in the presence and absence of tumor suppressor genes. Genes Dev 2001;15:3249–3262. [PubMed: 11751631]
42. Ding L, Getz G, Wheeler DA, et al. Somatic mutations affect key pathways in lung adenocarcinoma. Nature 2008;455:1069–1075. [PubMed: 18948947]
43. Navadgi-Patil VM, Burgers PM. The unstructured C-terminal tail of the 9-1-1 clamp subunit Ddc1 activates Mec1/ATR via two distinct mechanisms. Mol Cell 2009;36:743–753. [PubMed: 20005839]
44. Liu Q, Guntuku S, Cui XS, et al. Chk1 is an essential kinase that is regulated by Atr and required for the G(2)/M DNA damage checkpoint. Genes Dev 2000;14:1448–1459. [PubMed: 10859164]
45. Fang Y, Tsao CC, Goodman BK, et al. ATR functions as a gene dosage- dependent tumor suppressor on a mismatch repair-deficient background. EMBO J 2004;23:3164–3174. [PubMed: 15282542]
46. Bric A, Miething C, Bialucha CU, et al. Functional identification of tumor-suppressor genes through an in vivo RNA interference screen in a mouse lymphoma model. Cancer Cell 2009;16:324–335. [PubMed: 19800577]
47. Zighelboim I, Schmidt AP, Gao F, et al. ATR mutation in endometrioid endometrial cancer is associated with poor clinical outcomes. J Clin Oncol 2009;27:3091–3096. [PubMed: 19470935]
48. Zhou BB, Bartek J. Targeting the checkpoint kinases: chemosensitization versus chemoprotection. Nat Rev Cancer 2004;4:216–225. [PubMed: 14993903]
49. Fracasso PM, Williams KJ, Chen RC, et al. A Phase 1 study of UCN-01 in combination with irinotecan in patients with resistant solid tumor malignancies. Cancer Chemother Pharmacol. 2010

50. Syljuasen RG, Sorensen CS, Hansen LT, et al. Inhibition of human Chk1 causes increased initiation of DNA replication, phosphorylation of ATR targets, and DNA breakage. Mol Cell Biol 2005;25:3553–3562. [PubMed: 15831461]

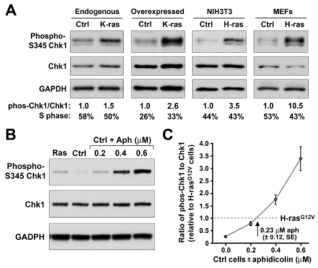


**Figure 1.**

Expression of oncogenic Ras mutants activates the ATR-Chk1 pathway. A, Western blot detection of Chk1-S345 phosphorylation in normal and oncogenic Ras-transformed cells. Control and K-ras$^{G12D}$- or H-ras$^{G12V}$-expressing murine embryonic fibroblast lines grown in defined media (*Materials and Methods*) were detected for Chk1-S345 phosphorylation by western blot. The increase in phospho-Chk1 over total Chk1 abundance was calculated on each blot relative to the levels observed in untransformed controls. GAPDH was additionally detected and quantified as a loading control. Flow cytometric quantification of S phase representation was performed in parallel by 45-minute BrdU incorporation and propidium iodide (PI) staining. B, Western blot detection of Chk1 phosphorylation in H-ras$^{G12V}$-transformed NIH3T3 cells in comparison to control cells treated for one hour with increasing concentrations of aphidicolin. C, Quantification of aphidicolin-stimulated Chk1 phosphorylation relative to average H-ras$^{G12V}$-stimulated phosphorylation. Western blots and quantification of Chk1 phosphorylation are representative of 3–4 independent experiments. Standard error (SE) bars are shown.

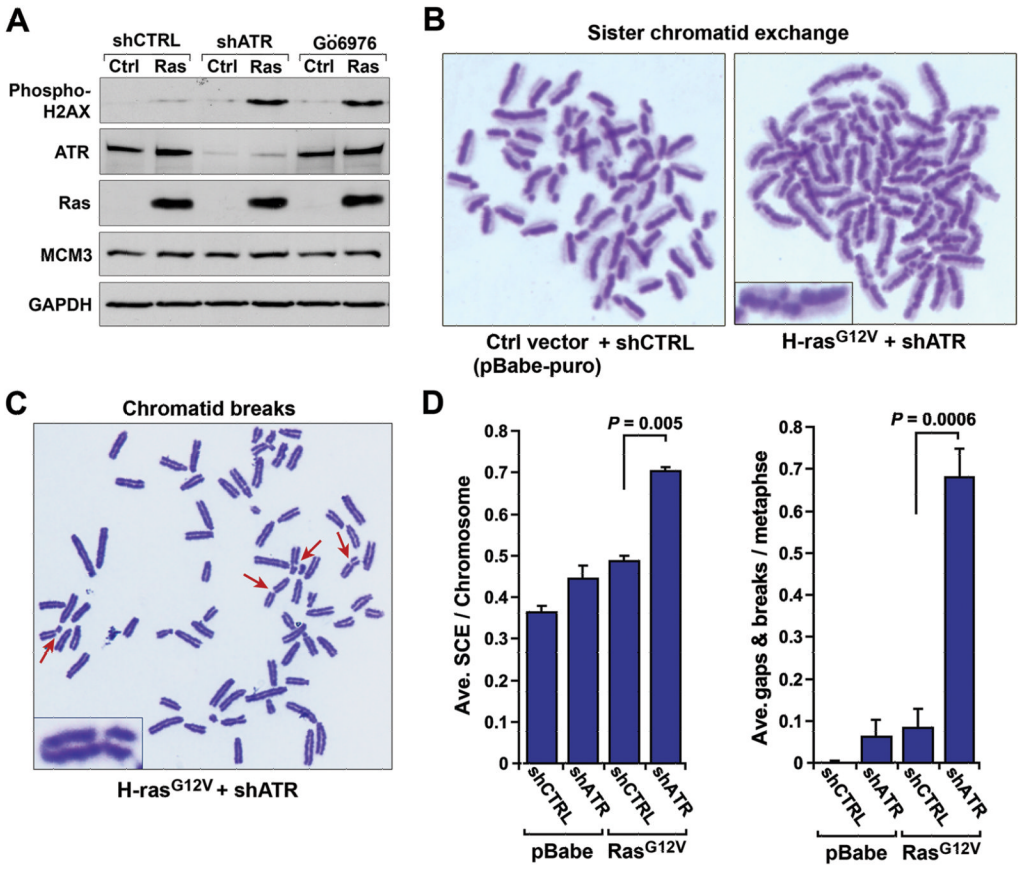


**Figure 2.**

Oncogenic Ras expression in combination with ATR-Chk1 pathway suppression leads to increased genomic instability. A, Increased H2AX phosphorylation upon ATR-Chk1 pathway suppression in combination with H-ras$^{G12V}$-transformation. ATR-Chk1 pathway was inhibited in H-ras$^{G12V}$-transformed or untransformed control cells (pBabe-puro transduced) via shRNA-mediated reduction of ATR expression (21) or three-hour treatment with the Chk1 kinase inhibitor Gö6976. Lysates were detected for H2AX phosphorylation by western blot; Ras and ATR levels were also detected with GAPDH and MCM3 as loading controls, respectively. Expression of shATR reduced ATR protein levels by 94% (untransformed control cells) and 81% (H-ras$^{G12V}$-transformed cells) in the experiment shown. These values were within the typical range of ATR reduction [86.9% ± 5.6 (S.E.) for untransformed controls, and 81.7% ± 1.8 (S.E.) for H-ras$^{G12V}$-transformed] and were sufficient to limit Chk1 S345 phosphorylation in response to low-dose aphidicolin (Supplemental Fig. 1). B and C, Representative SCE and chromatid break detection in H-ras$^{G12V}$-transformed cells following shRNA-mediated ATR reduction. Mitotic spreads for SCE and chromatid break detection were collected 48 hours after infection with lentiviruses that expressed the indicated shRNAs. D, Quantification of average SCEs and chromatid gaps and breaks following ATR suppression in H-ras$^{G12V}$-transformed and control cells. Data shown are derived from 3–5 independent experiments. For section D, standard error bars are shown and *P* values were calculated by the Student's t test.

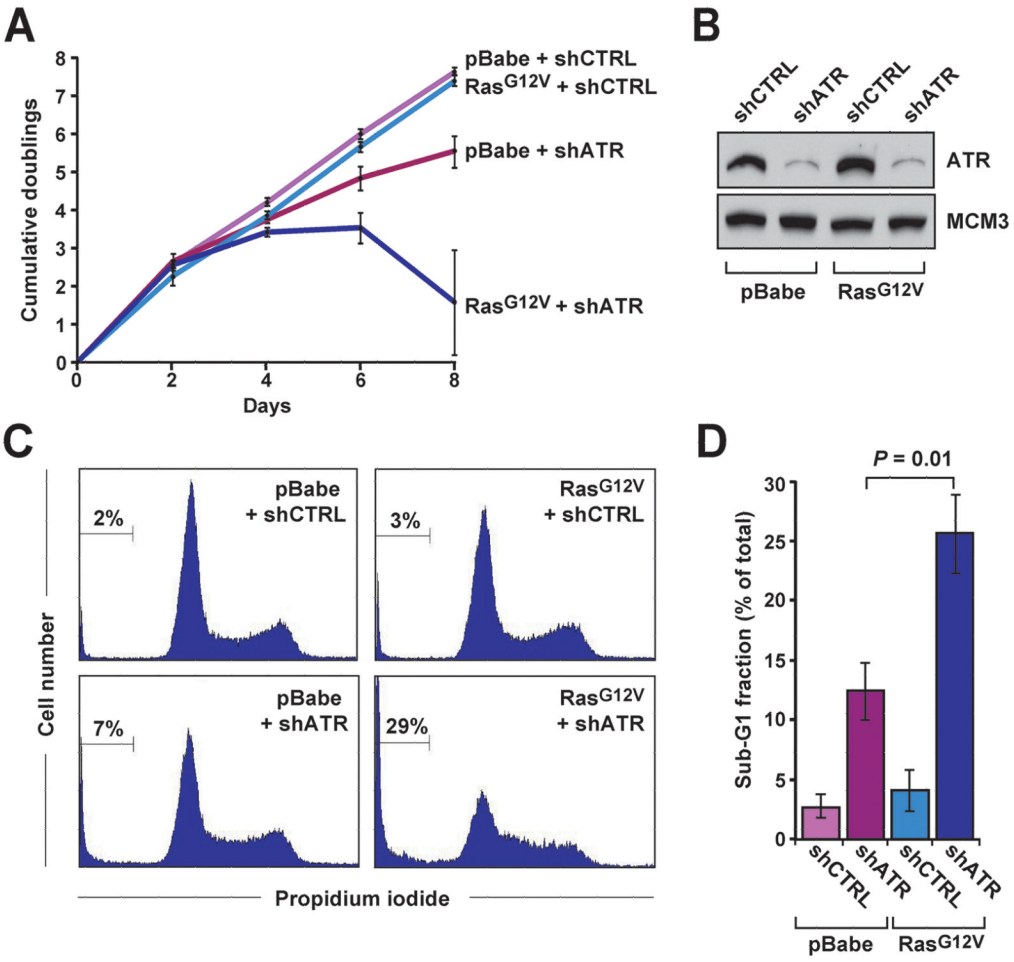


**Figure 3.**

ATR-Chk1 pathway hypomorphic suppression is synthetic lethal with oncogenic Ras-transformation. A, Proliferation of H-ras$^{G12V}$-transformed and control cells following ATR suppression. shRNA-mediated reduction of ATR was performed as described in Fig. 2. Cells were maintained at subconfluence by replating every two days, and cumulative population doublings were quantified over a total of 8 days. B, Western blot detection of ATR in lysates from control and H-ras$^{G12V}$-transformed cells following shRNA-mediated ATR suppression (Day 2). C, Cell cycle profiles (PI staining) of control and H-ras$^{G12V}$-transformed cells following ATR suppression. Sub-G1 populations are indicated (brackets). D, Quantification of average sub-G1 population frequency in H-ras$^{G12V}$-transformed and control cells with or without ATR suppression. Data shown are derived from 3–6 independent experiments. For sections A and D, standard error bars are shown and *P* values were calculated by the Student's t test.

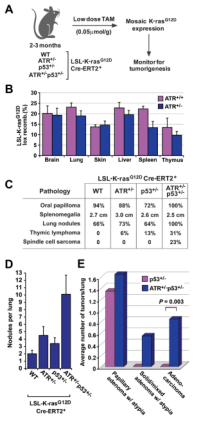


**Figure 4.**

ATR haploinsufficiency promotes K-ras$^{G12D}$-induced tumorigenesis. A, Schematic for ubiquitous mosaic activation of the lox-stop-lox (LSL) knock-in allele of K-ras$^{G12D}$ in ATR and p53 haploinsufficient mice. Recombination of the LSL-K-ras$^{G12D}$ allele was achieved through low-dose tamoxifen (TAM) activation of ubiquitously expressed Cre-ERT2 (28). B, Quantification of mosaic lox recombination of the LSL-K-ras$^{G12D}$ allele in various tissues. Real-time quantitative PCR (qPCR) analysis of genomic DNA was performed on tissues isolated from LSL-K-ras$^{G12D/+}$Cre-ERT2$^{+}$ mice (ATR$^{+/+}$, n=3 and ATR$^{+/-}$, n=6) five days after low-dose TAM treatment. Standard errors are indicated (bars). C, Tumorigenesis in ATR$^{+/-}$p53$^{+/-}$ and control mice following Cre-mediated mosaic expression of K-ras$^{G12D}$. The LSL-K-ras$^{G12D/+}$Cre-ERT2$^{+}$ mice analyzed were ATR$^{+/+}$ (n=18), ATR$^{+/-}$ (n=17), p53$^{+/-}$ (n=20), and ATR$^{+/-}$p53$^{+/-}$ (n=14). Tumors were identified upon necropsy or following IACUC-determined euthanasia endpoints, and the percentages of affected mice are shown. D, Average number of grossly-apparent lung nodules following mosaic activation of the LSL-K-ras$^{G12D}$ allele in ATR and p53 haploinsufficient mice. Nodules were quantified on fixed lungs isolated from low dose TAM-treated LSL-K-ras$^{G12D/+}$Cre-ERT2$^{+}$ mice with the indicated heterozygous deletions in ATR and p53 (n > 13 mice per genotype). E, ATR haploinsufficiency promotes K-ras$^{G12D}$-induced lung adenocarcinoma in p53 heterozygous mice. Quantification of adenoma subtypes and adenocarcinoma was performed on lung tissue isolated from low dose TAM-treated LSL-K-ras$^{G12D/+}$Cre-ERT2$^{+}$ mice with the additional genotypes indicated. Blinded analysis of hematoxylin-eosin stained serial sectioning (1 per 50 microns, 24-39 sections in total were analyzed per lung) was performed, and adenoma subtypes and adenocarcinoma were classified as described (29). Standard errors (bars) were calculated from three or more independent PCR reactions (section B) or from nodules per lung (n > 13 mice, section D). *P* value (section E) was calculated by Fisher's exact test.

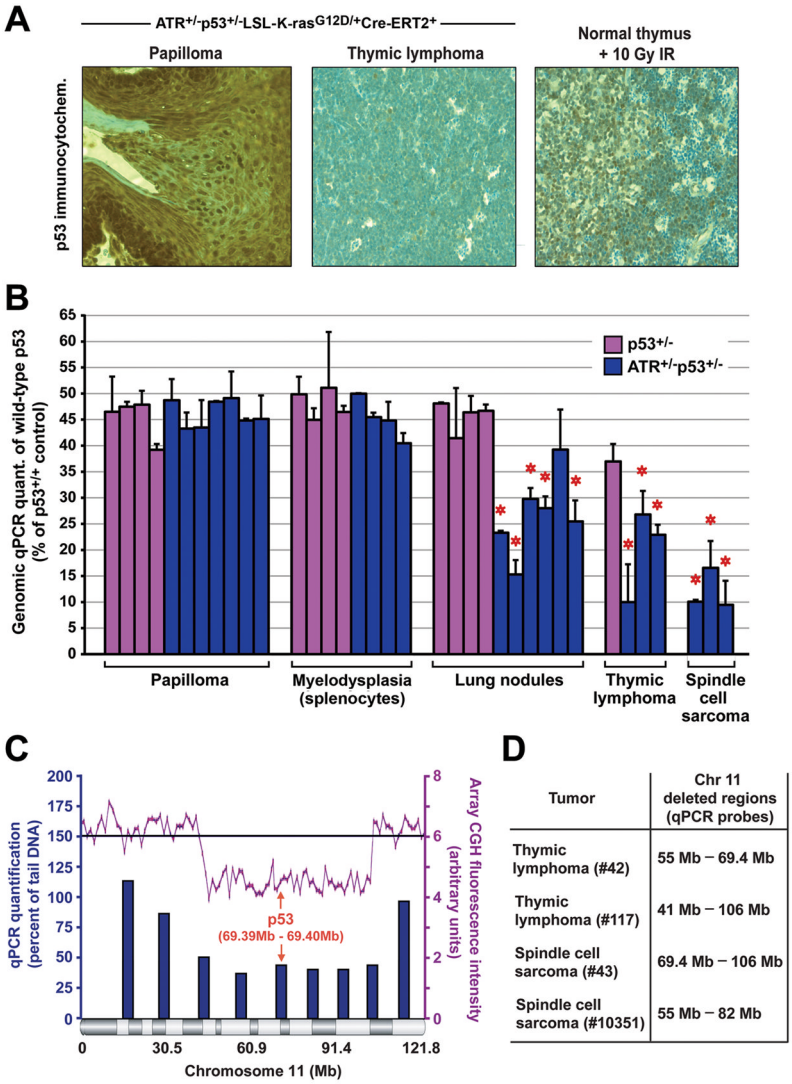


**Figure 5.**

ATR haploinsufficiency accelerates p53 LOH in K-ras$^{G12D}$-induced tumors. A, Detection of p53 by immunohistochemistry (IHC) in representative skin papilloma (n=2) and thymic lymphoma (n=4) isolated from low-dose TAM-treated ATR$^{+/-}$p53$^{+/-}$LSL-K-ras$^{G12D/+}$Cre-ERT2$^{+}$ mice. Normal thymus isolated from mice eight hours after exposure to 10 Gy ionizing radiation (IR) is shown as a positive control for p53 detection. Sections were stained in parallel using equivalent conditions. Nuclear p53 protein was not detected in spindle cell sarcomas isolated from ATR$^{+/-}$p53$^{+/-}$ mice (n=3, data not shown). B, Detection of genomic loss of the wild-type p53 allele in tumors isolated from TAM-treated p53$^{+/-}$LSL-K-ras$^{G12D/+}$Cre-ERT2$^{+}$ and ATR$^{+/-}$p53$^{+/-}$LSL-K-ras$^{G12D/+}$Cre-ERT2$^{+}$ mice. qPCR analysis of genomic DNA from tumors was performed as described in *Materials and Methods*. Wild-type p53 allele representation is shown relative to homozygous wild-type levels (p53$^{+/+}$). Standard errors (bars) were calculated from technical replicates. Tumor samples in which the wild-type p53 allele frequency was significantly reduced are indicated (red asterisks). Enrichment of K-ras$^{G12D}$ expressing cells in tumor isolates was determined by qPCR quantification of LSL-K-ras$^{G12D}$ lox recombination (Supplemental Fig. 5). C, Detection of intrachromosomal deletion of p53 by array CGH and qPCR analysis.

Representative qPCR regional quantification (blue bars) and array-CGH analysis of chromosome 11 (magenta line) on thymic lymphoma DNA isolated from a TAM-treated $ATR^{+/-}p53^{+/-}$LSL-K-$ras^{G12D/+}$Cre-$ERT2^{+}$ mouse. The location of the p53 gene is indicated. D, Deleted regions predicted by qPCR analysis of chromosome 11 in representative thymic lymphomas and spindle cell sarcomas from $ATR^{+/-}p53^{+/-}$LSL-K-$ras^{G12D/+}$Cre-$ERT2^{+}$ mice. Real-time primer sets (Supplemental Table 1) detecting chromosome 11 regions indicated in C were utilized in qPCR quantifications of tumor DNA and compared to pre-TAM treatment tail DNA. Regions that were selectively reduced in tumor DNA are shown.